Available online at www.sciencedirect.com
ScienceDirect
Ultrasonics Sonochemistry 15 (2008) 618–628
Ultrasonics SONOCHEMISTRY
www.elsevier.com/locate/ultsonch

Shock-wave model of acoustic cavitation

Sergei L. Peshkovsky, Alexey S. Peshkovsky *

Industrial Sonomechanics, LLC, 1505 St. Nicholas Ave., Suite 5B, New York, NY 10033, USA

Received 8 December 2006; received in revised form 5 July 2007; accepted 22 July 2007
Available online 7 August 2007

Abstract

Shock-wave model of liquid cavitation due to an acoustic wave was developed, showing how the primary energy of an acoustic radiator is absorbed in the cavitation region owing to the formation of spherical shock-waves inside each gas bubble. The model is based on the concept of a hypothetical spatial wave moving through the cavitation region. It permits using the classical system of Rankine–Hugoniot equations to calculate the total energy absorbed in the cavitation region. Additionally, the model makes it possible to explain some newly discovered properties of acoustic cavitation that occur at extremely high oscillatory velocities of the radiators, at which the mode of bubble oscillation changes and the bubble behavior approaches that of an empty Rayleigh cavity. Experimental verification of the proposed model was conducted using an acoustic calorimeter with a set of barbell horns. The maximum amplitude of the oscillatory velocity of the horns' radiating surfaces was 17 m/s. Static pressure in the calorimeter was varied in the range from 1 to 5 bars. The experimental data and the results of the calculations according to the proposed model were in good agreement. Simple algebraic expressions that follow from the model can be used for engineering calculations of the energy parameters of the ultrasonic radiators used in sonochemical reactors.

PACS: 43.35+d

Keywords: Acoustic cavitation; Acoustic wave; Cavitation bubble; Shock-wave; Shock-wave theory; Acoustic horn; Ultrasonic cavitation; Ultrasonic radiator; Ultrasonics

1. Introduction

In the design and calculation of powerful ultrasonic sources for sonochemical reactors, it is necessary to know the exact value of the intensity of the acoustic energy radiated into the working liquid. This information is usually obtained experimentally because no adequate physical model of acoustic cavitation that would allow one to obtain such data through calculation so far exists. The development of an adequate model of acoustic cavitation, although of great importance, has in the past been severely restricted by considerable mathematical difficulties connected with the necessity of finding numerical solutions of nonlinear equations describing the cavitation region (the visible region of large cavitation bubble population) [1]. Direct analytical solutions of these equations in different approximations do not give practical results suitable for the design of ultrasonic equipment [2,3].

Current literature on acoustic cavitation mainly tends to involve numerical models of spatio-temporal characteristics of the cavitation region [4–6]. Large number of theoretical acoustic cavitation models has been developed along with the corresponding methods of numerical analysis of such models. Further computer simulation-based investigations of acoustic cavitation have also been proposed, involving complex nonlinear physicomathematical models and including many aspects of spatial movement of cavitation bubbles in an acoustic field, spatial distribution of the characteristics of these fields in a liquid, interaction between the bubbles themselves, properties of acoustical flow, etc. [7–10]. Water is most frequently used for the experimental verification of such theoretical models.

* Corresponding author. Tel.: +1 (646) 267 2890.
E-mail address: alexey@sonomechanics.com (A.S. Peshkovsky).

1350-4177/$ - see front matter © 2007 Elsevier B.V. All rights reserved.
doi:10.1016/j.ultsonch.2007.07.006

No adequate explanation of the mechanism by which dissipation of the primary acoustic energy of a radiator occurs in a liquid at cavitation is, however, available from the literature. Additionally, no theoretical method permitting to calculate this energy in a manner adequate to the available experimental data currently exists. Meanwhile, the exact knowledge of the mechanisms by which the heating of a liquid in the presence of a cavitation-inducing acoustic wave occurs is quite important not only for the understanding of the related sonochemical processes, but also for the practical design parameter calculations that would permit constructing improved high-capacity ultrasonic radiators and reactors.

1.1. Visual observations of acoustic cavitation

Several authors provided common [11], high-speed [12] and stereoscopic high-speed [13] photographs of the cavitation region, obtained in the presence of relatively low-intensity acoustic fields. At these conditions, the cavitation region is located some distance away from the radiating surface and has a typical pattern similar to that of an electrical discharge.

Photographs of the cavitation region formed by powerful ultrasonic radiators have also been provided [14,15]. The diameters of the radiating surfaces of the radiators were greater than the sound wavelengths in the given liquid at the working frequencies. In these cases, plane acoustic waves are radiated into the liquid. The photographs show that at relatively low acoustic radiation intensity, the cavitation region is also located some distance away from the radiating surface, has an irregular pattern and is composed of thread-like collection of cavitation bubbles. As the radiation intensity goes up, however, the cavitation region approaches the radiating surface and grows in size. When the intensity reaches the value of, approximately, 1.5 W/cm^2, the cavitation region ''sits'' on the radiating surface and its shape becomes regular, resembling an upside-down circular cone. The so-called ''cone bubble structure'' begins to form. Further radiation intensity increases have little effect on the shape and position of the cone bubble structure. The photographs in the abovementioned studies show that at high radiation intensity the cone bubble structure is in contact with the radiating surface. Ref. [16] provides photographs of the radiating surface of a metal radiator which was utilized for a period of time to create high-intensity cavitation in a liquid. The surface of the radiator contains clear traces of metal degradation due to cavitation.

Therefore, it can be concluded with certainty that at high radiation intensities, acoustic cavitation starts at the surface of the acoustic radiator. This location in the liquid is known, according to theory, to have the lowest value of tensile strength due to the constant presence of adsorbed gas inclusions at the metal surface [2].

However, at low radiation intensities just above the cavitation threshold, the cavitation region in always formed at a significant distance away from the radiating surface, which contradicts the abovementioned theory. Clearly, the tensile strength of the liquid at any location away from the metal surface should be higher than near it, since the concentration of the preexisting bubbles (inceptions) that ''weaken'' the liquid at that location should diminish with time.

1.2. Justification for the shock-wave approach

At low radiation intensity, harmonic acoustic wave is not yet capable of inducing cavitation even at the weakest location in the liquid near the radiating surface. Formation of cavitation away from the radiating surface in this case can be explained by the effect of the increase of the planar acoustic wave front steepness during its propagation through a liquid. As a result of such increase, at some location in the liquid a discontinuity in the wave profile is formed. Since such discontinuity is physically not possible in a continuous media, a shock-wave with a steep front is formed as a result. This effect has to do with the acoustic radiation-induced nonlinearity of the compressible media properties and is very well known and documented [17].

This explanation, however, seems contradictory to the common shock-wave theory, since the attainable amplitude of vibration velocity of the radiating surface is always much lower than the speed of sound in the pure liquid and, therefore, the necessary conditions for the creation of such a discontinuity in the wave profile are not fulfilled. The explanation may, nevertheless, still be valid due to the following two considerations. It is well known that during propagation of an acoustic wave of slightly lower intensity than the cavitation threshold, an ensemble of tiny bubbles is formed in the liquid. This occurs due to the so-called ''rectified diffusion'' [2]. It is also well known that the speed of sound in a liquid containing gas bubbles is significantly lower than that in a pure liquid [18,19], and, under certain conditions, it may become similar to the amplitude of vibration velocity of the radiating surface.

It may, therefore, be considered that the bubbles formed in an acoustic wave due to rectified diffusion help forming a discontinuity in the profile of the acoustic wave at a location away from the radiating surface by significantly lowering the sound speed in the liquid. Further, at the location of the discontinuity in the acoustic wave, these tiny bubbles begin to undergo such rapid nonlinear movements that they loose dynamic stability and, consequentially, rapidly multiply forming the cavitation region.

The abovementioned observations and analysis formed the basis of the shock-wave model of acoustic cavitation described in this work. The model shows how the primary energy of an acoustic radiator causing the cavitation of liquid is absorbed in the cavitation region owing to the formation of spherical shock-waves inside each cavitation bubble. Calculation of the total energy absorbed in the cavitation region using the concept of a hypothetical spatial wave moving through the cavitation region is possible with this model using the classical system of the Rankine–

Hugoniot equations. Additionally, the proposed model makes it possible to explain some newly discovered properties of acoustic cavitation of water that occur at extremely high oscillatory velocities of the radiating surfaces.

2. Theory

Let us assume that an acoustic radiator emitting a plane-wave is used to generate cavitation in a liquid. The diameter of the radiator's output surface is comparable with the length of the acoustic wave in the liquid at the given frequency of vibrations. The frequency of the acoustic radiator vibrations should be considered to be much lower than the resonance frequency of the cavitation bubbles. We assume that the liquid always contains an equilibrium concentration of dissolved gas as well as some cavitation nuclei (tiny spherical bubbles filled with the gas) and, consequentially, the liquid possesses no tensile strength during rarefaction caused by the acoustic waves. As, for example, is indicated in Ref. [2], water that has not been purified of gas inclusions ruptures at the negative acoustic pressure of, approximately, 1 bar. The density of the liquid with the tiny cavitation nuclei is taken to be equal to the density of the pure liquid, ρ_f. Surface tension of the liquid and the presence of stable (non-cavitational) gas bubbles are neglected. Thus, within the framework of the model, only the so-called low-frequency transient gas cavitation is considered. We, additionally, assume the liquid to be non-viscous, non-compressible and non-volatile.

Let us represent acoustic cavitation in the liquid as a sequence of the following events. When an acoustic rarefaction wave of certain amplitude passes through a volume of the liquid, an explosive growth of cavitation nuclei occurs, leading to the formation of the gas-filled cavitation bubbles. Possible parameters of such rarefaction wave are described, for example, in [20]. A mixture of the spherical bubbles and the liquid is, therefore, formed. The gas dissolved in the volume of the liquid passes inside the free space formed by the bubbles. The density of the liquid, therefore, drops. At this point, the bubbles are so small, as compared with the acoustic wavelength, that the liquid/bubble mixture can be considered a continuous medium. The rarefaction wave phase is followed by a compression wave phase, whose passage results in a collapse of all gas bubbles, restoring the density of the liquid to ρ_f. The reverse diffusion of the gas back into the liquid during compression is insignificant and should be ignored. This particular stage of acoustic cavitation completes the total cavitation cycle and is further considered here in great detail, since it is this stage that is mainly responsible for the sonochemical effects of acoustic cavitation.

2.1. Oscillations of a single gas bubble

The problem of the liquid motion during the compression of an empty spherical bubble in liquid was solved by Rayleigh (see reviews [2,3]). On the basis of this solution and Ref. [17], the instantaneous pressure distribution in the liquid can be written as

$$p = p_\infty + \rho_f \frac{\dot{U}r + 2U^2}{\xi} - \rho_f \frac{U^2}{2\xi^4}. \tag{1}$$

Here, p_∞ is the pressure in the liquid at infinity, U is the velocity of the bubble boundary (wall), $\xi = R/r$, r is the current bubble radius, and R is the current radial coordinate. For the boundary of a gas-filled bubble at $\xi = 1$, the following equality must be met:

$$p_g = p_\infty + \rho_f \left(\dot{U}r + \frac{3}{2}U^2 \right). \tag{2}$$

Here, p_g is the gas pressure in the bubble. This expression is the well-known Noltingk–Neppiras equation (see reviews [2,3]).

For an empty bubble, taking $p_g = 0$ and $p_\infty = p_0$, integration of Eq. (2) gives Rayleigh's equations for the velocity of the bubble wall movement and the time of the bubble collapse:

$$u^2 = \frac{2p_0}{3\rho_f}\left(\frac{r_{in}^3}{r^3} - 1\right), \qquad \tau = 0.915 r_{in}\left(\frac{\rho_f}{p_0}\right)^{0.5}. \tag{3}$$

Here, p_0 is the static pressure, and r_{in} is the initial bubble radius.

From Eqs. (1) and (2), an expression for the instantaneous distribution of the pressure in liquid during the compression of a gas-filled bubble can be obtained:

$$p = p_\infty\left(1 - \frac{1}{\xi}\right) + \frac{p_g}{\xi} + \frac{\rho_f U^2}{2}\left(\frac{1}{\xi} - \frac{1}{\xi^4}\right). \tag{4}$$

Let us single out a spherical liquid volume that includes a gas bubble. The gas bubble/surrounding liquid system has a certain acoustic compressibility, which determines the velocity of the propagation of small perturbations or the velocity of sound in this volume. Using the linearized form of the Noltingk–Neppiras equation, one can obtain an expression for the velocity of sound in such a system, as it was done, for example, in the work [18]. The velocity of sound, with the abovementioned assumptions taken into account, is determined using the following expression:

$$c = \left(\frac{p_g}{\rho_f \alpha(1-\alpha)}\right)^{0.5}. \tag{5}$$

Here, α is the volumetric gas concentration in the singled-out liquid volume that includes a gas bubble. From Eq. (5) it can be seen that the velocity of sound at a given gas pressure in the bubble has a minimum at $\alpha = 0.5$. For example, at $p_g = 1$ bar the minimum velocity of sound $c_{min} = 20$ m/s. It should also be noted that the velocity of sound in the range $0.4 < \alpha < 0.6$ changes little.

A gas bubble is formed during the half-period of the liquid rarefaction in the acoustic wave. Under the abovementioned assumptions, this occurs at the moment when

the pressure in the liquid near the wall of a cavitation nucleus decreases to zero, i.e. the negative acoustic pressure is equal to p_0. At that point, the gas pressure in the formed bubble is also very small. Further, during the subsequent period of increase in the acoustic pressure, the bubble is compressed, and the gas pressure in it also increases. During the subsequent compression half-period, in the singled-out liquid volume near the gas bubble wall a spherical flow in the direction of the bubble center is formed, which is described by Eq. (4). From Eq. (5) it is seen that the velocity of sound for the singled-out system gas bubble/surrounding liquid depends on the gas pressure in the bubble p_g and the value of coordinate ξ, along which the boundary of the singled-out volume passes. If we start reducing the singled-out volume, while the radius of the bubble and the gas pressure in it are constant, the velocity of sound in this system will fall to a certain limit and then will grow again. This means that in the considered spherical volume near the moving wall of the bubble, there is a critical spherical region, where the sound velocity, c_{min}, is at the minimum at a given gas pressure in the bubble, p_g. The position of this region is determined from the condition $0.4 < \alpha < 0.6$. It is located close to the bubble wall in the coordinate range $1.18 < \xi < 1.35$. For the simplicity of further analysis of Eq. (4), it is taken that the velocity of the flow of the liquid particles in the critical region is equal to the velocity of the bubble wall movement, U.

In the model being considered, it is assumed that when the gas bubble/surrounding liquid system is compressed by the external pressure, p_∞, the velocity of the flow of the liquid particles in the critical region near the bubble wall increases to such a degree that at a certain gas pressure in the bubble, p_g, it reaches the minimum velocity of sound in the system under consideration, i.e. $U = c_{min}$.

At a ratio of the initial radius of an empty bubble to its current radius, $r_{in}/r = 2$, and static pressure, $p_0 = 1$ bar, the value of $U \approx 21$ m/s reached according to Eq. (3) is indeed close to $c_{min} = 20$ m/s.

Let us represent the pressure at infinity as a sum of the static and the acoustic (excessive) pressures, $p_\infty = p_0 + p'_\infty$ and transform Eq. (4) taking into account that $U = c_{min}$:

$$p = (p_0 + p'_\infty)\left(1 - \frac{1}{\xi}\right) + \frac{p_g}{\xi} + 2p_g\left(\frac{1}{\xi} - \frac{1}{\xi^4}\right). \quad (6)$$

This expression describes the extreme condition of equilibrium of the system. Eq. (6) shows that during compression of the flowing liquid, in the vicinity of the gas bubble a pressure impulse is formed, which is stationary with respect to the bubble wall. The amplitude of the excess pressure in this impulse is $p - p_0 = 1.4p_g + 0.5\delta p'_\infty$, where $\delta p'_\infty = (p'_\infty - p_0)$. This value is reached at the coordinate $\xi \approx 2$ located upstream from the critical region. As we show below, the quantity, $\delta p'_\infty$, does not need to be considered for small oscillation velocities of acoustic radiators.

When the velocity of the bubble wall motion exceeds the minimum velocity of sound, $U > c_{min}$, the equilibrium state described by Eq. (6) becomes destroyed, and the pressure in the liquid at the bubble wall downstream from the critical region decreases to p_0. The velocity of the bubble wall movement also reduces because the driving pressure difference decreases. At the same moment, the excessive pressure amplitude in the impulse increases stepwise up to the value $p - p_0 = 1.4p_0 + 0.5\delta p'_\infty$, since the boundary condition in Eq. (2) is changed and the pressure near the bubble wall becomes $p_g = p_0$. This occurs because the bubble pressure signal does not penetrate upstream from the bubble wall when $U > c_{min}$.

Due to destruction of the dynamic equilibrium (retardation of a part of the flow), the pressure impulse located in the liquid upstream from the critical section disintegrates and begins to move relative to the bubble boundary in the form of a converging spherical wave. The supposed instantaneous distribution of excessive pressure in the impulse near the gas bubble wall at $U = c_{min}$ is shown in Fig. 1.

Phenomena similar in essence are observed during the breakup of arbitrary pressure discontinuity in a gas, during hydraulic impact, and during the flow of gases and gas–liquid mixtures through nozzles. See, for example, the works [5,6], as well as the studies on Laval nozzles and water hammers.

In accordance with the assumed form of pressure distribution in a converging spherical wave shown in Fig. 1, the excessive pressure at the bubble wall first increases smoothly up to the value of $p - p_0 = 1.4p_g + 0.5\delta p'_\infty$, and, accordingly, the gas pressure inside the bubble increases smoothly (isothermally) as well. Then, when an abrupt excess pressure jump (up to the value of $p - p_0 = 1.4p_0 + 0.5\delta p'_\infty$) approaches the bubble wall, a spherical shock-wave is formed in the gas inside the bubble. The pressure jump itself, evidently, is equal to $1.4(p_0 - p_g)$. After focusing in the center of the gas bubble, the spherical shock-wave is reflected, and the bubble "explodes" from the

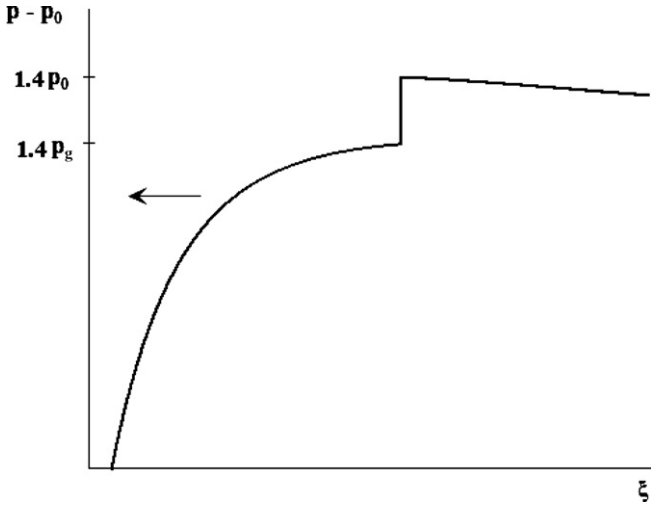

Fig. 1. Instantaneous distribution of the excessive pressure in the liquid near the cavitation bubble wall at $U > c_{min}$ is shown. The quantity $\delta p'_\infty$ is not taken into account.

inside, breaking up into small fragments. The collapse of the gas bubble or, more precisely, its shock destruction occurs. Gas pressure and temperature inside the bubble during the focusing and the subsequent reflection of the shock-wave reach very large, albeit theoretically restricted, values [17]. When the collapse of the gas bubble is completed, its small fragments are left in the singled-out liquid volume, which are equal in size to the original cavitation nuclei, and the density of the singled-out liquid volume becomes close to the initial liquid density, ρ_f. As we show below, when the oscillation velocities of the ultrasonic radiators reach very high values, cavitation may follow a different mechanism, which does not involve breaking the gas bubbles up into small fragments, but rather exhibits bubble behavior approaching that of an empty Rayleigh cavity.

This approach permits easily eliminating a seemingly clear contradiction that follows from the Noltingk–Neppiras equation: how can a gas-filled bubble implode with a very high rate if the gas pressure inside the bubble during compression rapidly increases, while the rate of the gas diffusion from the bubble, according to [2,3], is negligible. In the proposed model, the gas bubble does not implode in the literal sense of the word, but is destroyed by a spherical shock-wave reflected after focusing in its center. The presence of a well-known phenomena accompanying acoustic cavitation, such as sonoluminescence, erosion and dispersion of solids, emulsification of liquids, etcetera, can be well explained from this point of view. Additionally, the mechanism of the dissipation of the primary acoustic energy during the liquid cavitation becomes clear. This is the mechanism of the heating of a compressible medium in a shock-wave, which is well described in the literature (see, for example, [17]).

2.2. Cavitation region

During the rarefaction of a liquid in an acoustic wave, a mixture of a great number of spherical gas bubbles with the liquid (cavitation region) is formed. Let us call this gas–liquid mixture present in the cavitation region, the "continuum". In the previous section, the course of events during the collapse of a single bubble in some small volume of liquid was described. To extend these events over the entire continuum, a transition to spatial description is necessary. At that, the results of this transition must depend neither on the dimensions and the form of the continuum itself nor on the sizes and the spatial distribution of the bubbles in it.

During the compression stage, an acoustic radiator creates a pressure impulse in the liquid beyond the continuum in the form of a plane acoustic wave. Since the velocity of sound in the continuum is finite, the collapse of a multitude of gas bubbles located arbitrarily in the continuum must also occur simultaneously only in some narrow layer, as the impulse of the acoustic pressure approaches it, i.e. it must have a wave character. In the current model representation, the result of the superposition of many spherical shock-waves, which are formed near each gas bubble during its collapse in a narrow layer of the continuum, is a spatial wave (SW) moving through the continuum. Such a representation is the most exact and visual way of extending the events occurring during a single gas bubble collapse, over the entire continuum.

In the real situation, the cavitation region in a liquid may take very complex, branched shapes. The spatial distribution of bubbles in the region also may be quite nonuniform and the sizes of the bubbles may vary. When the transition to the presented spatial description of cavitation is made, for the results to be independent of the shape of the cavitation region as well as of the spatial distribution and the sizes of the bubbles, in our fundamental equations we will further utilize hypothetical physical parameters related to the cavitation region as a whole. In other words, instead of operating with local values of density, changes in internal energy and so on, we will use the values averaged over the whole cavitation region. As demonstrated below, these values disappear when further modifications of the fundamental equations are made.

The experimental investigations of acoustic cavitation described below conducted for the verification of the presented model were carried out using calorimetry of the entire environment and, therefore, provide only the spatially averaged values due to a relatively high thermal conductivity of the liquid. Therefore, the final purpose of the calculations following this model is the determination of a cumulative value of the changes in the internal energy of the environment, as a result of acoustic cavitation.

The spatial wave (SW) described above has a bore wave-like character, however, the continuum density and pressure inside the SW front change stepwise. This occurs because the cavitation bubbles collapse inside its front, following the process outlined in Section 2.1. The presence of such a wave is the final stage of acoustic cavitation, within one cycle of the continuum rarefaction–compression. In other words, according to the model, it is assumed that the collapse of the gas bubbles occurs inside a relatively narrow front of a hypothetical SW, being formed and moving through the continuum in each compression half-period of an acoustic radiator.

The width of the SW front, inside which the collapse of the bubbles and the change of the continuum density occur, can be estimated as the product of the empty bubble collapse time, according to Eq. (3) and the wave front movement velocity with respect to the continuum, $h = c\tau$. A rough estimate for the wave front movement velocity can be made using expression (5). Then, at $\alpha = 0.1$ (taken from the literature data [20] and characteristic for the initial stage of acoustic cavitation) we obtain $h \approx 3r_{in}$. According to the estimation performed in the work [2], the maximum radius of a gas bubble in water does not exceed 2×10^{-4} m, since larger bubbles rapidly rise to the surface. Hence, the value is: $h \leqslant 6 \times 10^{-4}$ m, which is smaller than the dimensions of the continuum itself by many orders of magnitude. Thus, the specified wave has a front that is very narrow

relative to the dimensions of the entire continuum. Getting over this barrier, therefore, the physical parameters of the continuum change stepwise.

It is necessary, further, to establish a relation between the continuum parameters ahead of and behind the SW front, as well as the relationship between these parameters and the oscillatory velocity of an acoustic radiator. It is important to note that the velocity of the specified wave can be lower than the velocity of sound in the continuum.

The SW moving through the continuum is not only a physical abstraction used for the construction of the model, but can, apparently, exists in reality. In this case, however, we are not faced with an ordinary shock-wave, which arises in a compressible continuum when the piston movement velocity is higher than the sound velocity in the continuum. Such shock-waves in a gas–liquid suspension obtained by bubbling a gas through a liquid are described in detail in literature [18]. Here, it is assumed that in a gas–liquid suspension formed as a result of the liquid rarefaction in an acoustic wave, another type of bore wave-like shock-waves may exist, which is associated with the radial movement of the liquid in the vicinity of each bubble.

It is well known that when a jump (discontinuity) of a physical quantity arises in a compressible continuum, a solution should be sought using the general conservation laws in the form of the Rankine–Hugoniot equations [17]. These equations reflect the ratios of the steady-state physical parameters of the compressible continuum before and after the passage of the shock-wave front. Additionally, there appears a possibility to analytically calculate the values of important parameters, without considering in detail the transient processes inside the SW front, which are connected with the complex kinetics of a collapsing gas bubble.

Let us introduce the following designations: p_h is the pressure in the liquid phase of the continuum near the bubble wall after the SW passage; p_l, $\rho_l = \rho_f(1-\alpha_l)$, α_l are, respectively, the pressure in the liquid phase of the continuum near the bubble wall, the density and the volumetric gas content of the continuum before the SW passage. A scheme of the continuum flow is presented in Fig. 2. It is assumed that a SW moves through the continuum, and that the gas bubbles collapse inside the narrow front of this wave. Also shown in this figure is the supposed pressure profile in the continuum.

Fig. 3 shows the supposed processes occurring in one cycle of the acoustic cavitation of liquid. The pressure in the liquid phase of the continuum near the gas bubble wall in an arbitrary state is plotted on the ordinate, and the continuum specific volume is plotted on the abscissa. Line 1 represents the rarefaction of the continuum with cavitation nuclei in an acoustic wave. Line 2 represents a nonlinear process of the growth of cavitation bubbles in the rarefaction wave. Line 3 represents a preliminary compression of the continuum in an acoustic wave (for a single gas bubble, this corresponds to a rise in the gas pressure in the bubble on the smooth section of a converging spherical wave, as described in Section 2.1). Line 4 represents the continuum's transition from one state to the other when the SW passes (for a single gas bubble, this corresponds to a rise in the gas pressure in the bubble on the steep section of a converging spherical wave, as described in Section 2.1). In this scheme, it is assumed in advance that the velocity of the SW movement through the continuum can be lower than the sound velocity in the continuum itself ahead of SW. Additionally, the SW front itself serves as a source of the acoustic wave, propagating forward in the direction of the shock-wave movement. In this connection, there is a preliminary compression of the continuum, and line 4 begins above the abscissa axis.

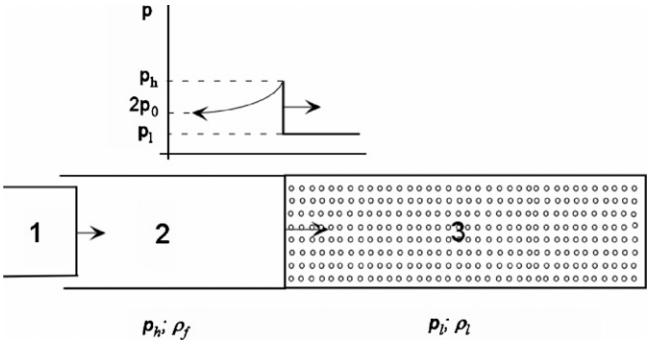

Fig. 2. Schematic of the continuum's flow during compression is shown (1 – acoustic radiator, 2 – flow region after the SW passage, 3 – flow region before the SW passage).

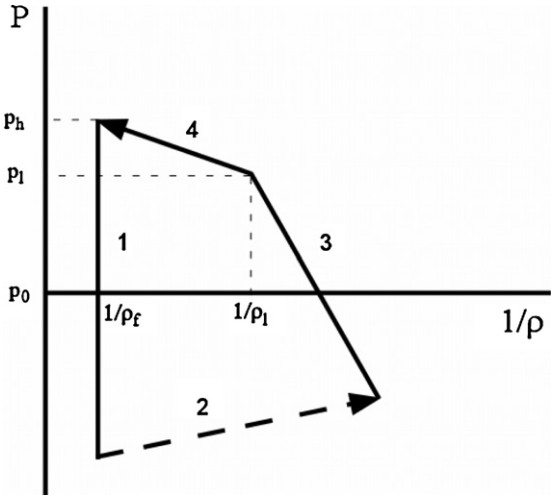

Fig. 3. Processes occurring during acoustic cavitation are illustrated. Line 1 represents the rarefaction of the continuum with cavitation nuclei in an acoustic wave, line 2 represents a nonlinear process of the growth of cavitation bubbles in the rarefaction wave, line 3 represents a preliminary compression of the continuum in an acoustic precursor wave, line 4 represents the continuum transition from one state to the other when the SW passes.

This kind of an acoustic wave is called a precursor. The precursor does not cause the collapse and disintegration of the bubbles because of a small value of its amplitude. Similar representations are used for initially loose or porous environment. In such environment, during the compression

phase, the shock-wave front is formed only due to the parameters of the compression process itself since this environment tends to change the specific volume of pores (cavities) abruptly (stepwise) under pressure [22–24].

Let us introduce the following additional designations: $p_l = p_0 + p'_l, p_h = p_0 + p'_h$; p'_l and p'_h are the excessive pressures in the liquid phase of the continuum near the bubble wall before and after the SW passage, respectively; u_l and u_h are the continuum flow velocities relative to SW before and after its passage, respectively; e_l and e_h are the specific internal energy of the continuum before and after the SW passage, respectively; v is the current oscillatory velocity of an acoustic radiator; v_t is the critical oscillatory velocity of an acoustic radiator, which corresponds to the cavitation onset (cavitation threshold). Note that a stepwise increase in the continuum density from ρ_l to ρ_f at the SW front corresponds to a change in pressure from p_l to p_h. The relative movement of the liquid and the gas bubbles is neglected.

Let us now write the system of conservation equations (Rankine–Hugoniot equations) for the continuum parameters on both sides of the SW front:

$$\begin{aligned}
&\rho_l u_l = \rho_f u_h,\\
&p'_l + \rho_l u_l^2 = p'_h + \rho_f u_h^2,\\
&\frac{p_0 + p'_l}{\rho_l} + \frac{u_l^2}{2} + e_l = \frac{p_0 + p'_h}{\rho_f} + \frac{u_h^2}{2} + e_h,\\
&v - v_t = u_l - u_h.
\end{aligned} \tag{7}$$

The fourth equation of system (7) shows that a change in the continuum's movement velocity getting over the SW front is equal to the excessive oscillatory velocity of an acoustic radiator, which exceeds the critical value, v_t.

This system of equations can be transformed to the following form:

$$\begin{aligned}
&I = \frac{(2p_0 + p'_l + p'_h)}{2}(v - v_t),\\
&\eta_l = \frac{(v - v_t)^2}{p'_h - p'_l}.
\end{aligned} \tag{8}$$

Here, $I = (e_h - e_l)\rho_f u_h$ is the flux density of the energy dissipated inside the SW as a consequence of the dissipation processes related to the bubble collapse and $\eta_l = \alpha_l/\rho_l$ is the volume of all cavitation bubbles per unit mass of the liquid phase of the continuum before the SW passage.

The average flux density of the acoustic energy (acoustic energy intensity) absorbed in one acoustic wave period can be presented in the following way:

$$I_a = \frac{\omega}{2\pi}\int_0^{\pi/\omega} |I\sin(\omega t)|\mathrm{d}t = I/\pi. \tag{9}$$

3. Setup of the equations for the experimental verification

To experimentally verify resulting Eq. (8), it is necessary to determine the values of p'_h, p'_l, η_l and v_t.

3.1. Small oscillatory velocities of acoustic radiator

From Eq. (6) and the analysis given in Section 2.1, it follows that the maximum excessive pressure at the SW front is equal to $p'_h = 1.4p_0 + \delta p'_\infty$. As mentioned above, the liquid utilized for the construction of the theoretical model, does not possesses tensile strength during rarefaction. Consequentially, the explosive growth of the cavitation nuclei and their conversion into gas bubbles in the rarefaction wave takes place at the negative pressure equal to the static pressure, $p'_\infty = p_0$. It is possible to assume that for small oscillation velocities of the acoustic radiator near the cavitation threshold a symmetry of acoustic pressure amplitudes during the half-periods of compression and rarefaction is conserved. Consequentially, in this case, $\delta p'_\infty = 0$ and $p'_h = 1.4p_0$. It will be shown below that for large radiator oscillatory velocities it is no longer possible to ignore the quantity $\delta p'_\infty$. Note that the value of $p'_h \approx 1.4p_0$ actually corresponds to the threshold of water cavitation, at least, in its initial stage. This fact was experimentally established in [21].

Above, it was assumed that during the rarefaction of a liquid in an acoustic wave, all gas dissolved in a unit volume of the liquid passes into the bubbles formed in this volume. The oscillations of the gas bubbles before the onset of their collapse are isothermal, and the mass of the gas in them does not change. From the analysis of Eq. (6) given in Section 2.1, it follows that $p'_l = 1.4p_g$, hence, the condition $p_0\eta_0 = 0.71p'_l\eta_l$ must be met. Here, η_0 is the equilibrium volume of gas dissolved in a unit mass of the liquid at the pressure, p_0.

The quantity v_t is the critical oscillatory velocity of an acoustic radiator, which corresponds to the cavitation threshold. In view of the conditions described above, one can assume that for a plane acoustic wave, $(v_t)_{rms} = 0.71p'_\infty/\rho_f c_f = 0.71p_0/\rho_f c_f$.

It should be borne in mind that the value of v_t in each particular experimental case can be different from the specified theoretical value. This is connected with the fact that the practical value of v_t depends on a large number of different parameters of liquid (physical nature, purity degree, gas content, volatility, sample preparation history, etc.). Besides, v_t also depends on the conditions of the conducted measurements (frequency of ultrasound, degree of isolation from external radiation, temperature, etc.).

From the second equation of system (8) we obtain:

$$p'_l = \frac{1.4p_0^2\eta_0}{\eta_0 p_0 + 1.42(v - v_t)_{rms}^2}. \tag{10}$$

Now from the first equation of system (8) in view of Eqs. (9) and (10) we obtain the final equation for the average flux density of the acoustic energy (intensity of acoustic energy) absorbed in the cavitation region:

$$I_a = 0.76p_0\left[1 + \frac{0.41p_0\eta_0}{\eta_0 p_0 + 1.42(v - v_t)_{rms}^2}\right](v - v_t)_{rms}. \tag{11}$$

For the initial stage of acoustic cavitation, at a small value of $(v - v_t)_{rms}$, the final equation is as follows:

$$\frac{I_a}{p_0} = 1.07(v - v_t)_{rms}. \quad (12)$$

It is important to point out that in Eqs. (11) and (12) the quantities related to the spatial distribution of gas bubbles in the continuum and their size, as well as the form and shape of the continuum itself are not present.

3.2. High oscillatory velocities of acoustic radiator

From the main system of Eq. (7), one can obtain the expression for the SW velocity relative to the unperturbed continuum, $u_l = [(p'_h - p'_l)/\rho_f \alpha(1-\alpha)]^{0.5}$. The ratio of u_l to the sound velocity, c, in the continuum according to Eq. (5), using Eq. (10) and taking into account that $p_g = 0.71p'_l$, can be written as

$$\frac{u_l}{c} = \left(\frac{p'_h - p'_l}{p_g}\right)^{0.5} = \left(\frac{2(v - v_t)^2_{rms}}{p_0\eta_0}\right)^{0.5}. \quad (13)$$

From this expression, it is seen that at $(v - v_t)_{rms} \geqslant 1$ m/s, the SW movement must become supersonic, making it a real shock-wave in the classical sense. When the SW movement is supersonic, a precursor is absent because it is absorbed by the faster shock-wave. The density and the pressure of the gas inside the bubbles in this case are initially small since they are not compressed beforehand by the precursor. From the analysis of Eq. (10), it is seen that at $(v - v_t)_{rms} > 3$ m/s the gas pressure in such bubbles becomes approximately an order of magnitude lower than the static pressure, p_0, and continues to decrease. A spherical shock-wave in rarefied gas inside such a bubble is not formed and, accordingly, the bubble does not break up into small fragments as a result of the collapse. The behavior of the bubble becomes close to the behavior of an empty Rayleigh cavity.

It is also important to keep in mind that the minimum width of the shock-wave front in a gas is on the order of the molecule free path [17]. At a normal density of the gas, this distance is about 10^{-7} m. With a decreasing gas density, this distance increases proportionally and becomes close to the characteristic size of the bubble itself 10^{-5} m. Under these conditions, a spherical shock-wave inside the bubble cannot be formed, and the bubble is compressed like a Rayleigh cavity.

At the final stage of the collapse of the bubble, the gas pressure in it increases to such a degree that it can hold back the liquid's pressure. At that, the pressure and temperature of the compressed gas can reach very high values (theoretically unrestricted under the assumptions of this model [17]). In this case, at the excess pressure, $p'_h = 1.4p_0$, the continuum behind the SW is a gas–liquid suspension with some density $\rho_h = \rho_f(1 - \alpha_h)$. If the conditions identified in the beginning of Section 2, assumed for the construction of the model, are to be met, the continuum behind the front of SW is additionally compressed by the acoustic radiator until density ρ_f is reached. This corresponds to a pressure increase at the SW front up to the value of $p'_h = 1.4p_0 + \delta p'_\infty = 1.4p_0 + 0.5c_h^2\delta\rho = 1.4p_0 + 0.5c_h^2\rho_f\alpha_h$, where $\delta\rho = \rho_f - \rho_h = \rho_f\alpha_h$ is the additional increase in the continuum's density behind the SW front, necessary to reach the quantity ρ_f, and c_h is the speed of sound in the gas–liquid suspension with density ρ_h. For high oscillatory velocities of acoustic radiator similar to the sound speed in the continuum, $p'_h = 1.4p_0 + \rho_f\alpha_h v^2_{rms}$, since in this case it can be taken that $c^2 = 2v^2_{rms}$.

The value of v_t is neglected. Since $\delta p'_\infty$ should be taken into account only at high v and the second term of Eq. (11), which corresponds to the excessive pressure p'_l, is negligible, we leave it unchanged. Let us now write Eq. (11) in the final form in view of Eq. (9):

$$I_a = 0.76p_0\left[1 + \frac{0.41\eta_0 p_0}{\eta_0 p_0 + 1.42(v - v_t)^2_{rms}} + \frac{0.29\rho_f\alpha_h v^2_{rms}}{p_0}\right](v - v_t)_{rms}. \quad (14)$$

4. Interpretation of the experimental results provided in Ref. [21]

A large series of experiments aimed at studying acoustic cavitation of water at low oscillatory velocities of acoustic radiator is presented in the work [21]. Experiments were conducted in degassed water with the concentration of the dissolved air equal to 30% of the nominal concentration in the equilibrium state at the room temperature and the normal static pressure.

For the interpretation of these data, let us introduce the following designations: $\sum I_a = 0.5(p'_h)^2\gamma = p_0^2\gamma$ is the total intensity of the acoustic energy radiated into water; $I_{a0} = 0.5(p'_h)^2\gamma_f = p_0^2\gamma_f$ is the intensity of the acoustic energy propagating beyond the bounds of the cavitation region. Here, γ is the specific acoustic radiation admittance of the continuum, $\gamma_f = 1/\rho_f c_f$. The difference of these intensities is the intensity of the acoustic energy absorbed in the cavitation region. Thus, when compared with the theoretical results of the given model, the experimental values of γ for each oscillatory velocity obtained in [21] were recalculated by the following expression:

$$\frac{I_a}{p_0} = (\gamma - \gamma_f)p_0. \quad (15)$$

In representing the data of the work [21], the values of $(v_t)_{rms}$ were determined directly from the experimental plots of this work at the point of characteristic inflection.

5. Experimental setup

To measure the acoustic energy absorbed in a cavitating liquid at an increased static pressure p_0, an acoustic calorimeter described in [25] was used. The operating frequency of the magnetostrictive transducer was 17.8 kHz. Acoustic radiators were a set of the barbell horns with equal-size

radiation surfaces, which were designed using the method described in [25]. The radiating surfaces' diameters were 60 mm and thus provided the generation of plane acoustic waves in water at the given frequency. The oscillatory velocity of the acoustic radiators reached very high values. The highest oscillatory velocity amplitude achieved in the experiments was $v = 17$ m/s. Static pressure in the calorimeter was produced with compressed nitrogen. Settled tap water at 20 °C was used. The static pressure, p_0, varied in the range of 1.0–5.0 bar; the water density, $\rho_f = 998$ kg/m^{-3}; sound velocity in the water, $c_f = 1500$ m/s; the volume of air dissolved in unit mass of water, $\eta_0 = 2.2 \times 10^{-5}$ m^3/kg. Each experimental point shown on the plots was obtained as a mean value of 10 measurements.

6. Experimental results

Experimental data for small oscillatory velocities of an acoustic radiator, v, and different static pressures, p_0, are shown in Fig. 4. The values of v_t used in the treatment of these experimental data were calculated from the expression $(v_t)_{rms} = 0.707 p_0/\rho_f c_f$ for different static pressures. Also shown in this figure are the experimental data from [21] for ultrasound frequencies of 19 and 28 kHz, closest to the frequency 17.8 kHz used in the present work, which are interpreted by Eq. (15). The values of the cavitation threshold obtained from the corresponding plots of [21] for both frequencies $(v_t)_{rms} = 0.08$ m/s. Fig. 4 also shows the theoretical lines calculated from Eqs. (11) and (12), which are represented by the solid and the dotted lines, respectively.

A good agreement between the theoretical lines themselves and the experimental data with these lines at small values of v can be clearly seen. With increasing $(v - v_t)_{rms} > 0.2$ m/s, the experimental points diverge from the straight line plotted from Eq. (12) and approach the line plotted from Eq. (11).

Fig. 5 shows the experimental results for all oscillatory velocities of the acoustic radiator, v, which were used in the experiments at normal static pressure, $p_0 = 1$ bar. Also shown in this figure are the theoretical lines plotted from Eqs. (11) and (14). From Fig. 5 it is seen that at intermediate values of v the experimental points are located near practically coincident lines plotted from Eqs. (11) and (14), which are represented by the dotted and solid lines, respectively.

At high oscillatory velocities, $(v - v_t)_{rms} > 3$ m/s, the specified theoretical relationships diverge, and the experimental points are located according to a more general relationship (14) at $\alpha_h = 0.4$. It can be seen that the theoretical and the experimental data are in good agreement up to the highest values of the oscillatory velocity, v.

A spread of the experimental points on the curve in Fig. 5 in the region $2 \text{ m/s} < (v - v_t)_{rms} < 3$ m/s is also observed. Here, the beginning of the divergence of the theoretical curves 1 and 2 is observed as well. These phenomena are, apparently, associated with the establishment of the supersonic regime of the SW movement and a considerable decrease in the gas pressure in the bubbles. The indication of the possibility of the supersonic regime of radiation at acoustic cavitation was first made in the work [26]. The phenomenon itself was called the second threshold of acoustic cavitation. The region located over the second threshold at $(v - v_t)_{rms} > 3$ m/s was called the region of acoustic supercavitation. The closest related known phenomenon is called hydrodynamic supercavitation and is described, for example, in [27].

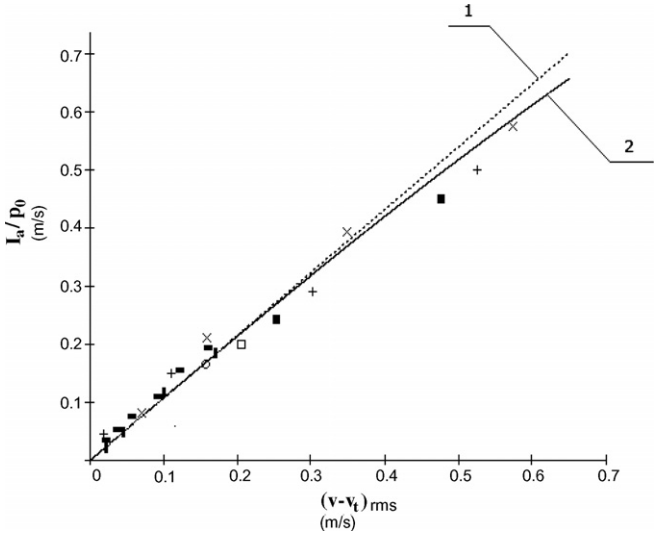

Fig. 4. Intensity of acoustic energy absorbed in water at cavitation is shown as a function of the excessive oscillatory velocity of an acoustic radiator for pressures of × – 1 bar, + – 2 bar, ■ – 3 bar, □ – 4 bar, ○ – 5 bar, at frequencies of ▌ – 28 kHz and ▬ – 19 kHz from the work [21]. Line 1 is plotted from Eq. (12); line 2 is plotted from Eq. (11).

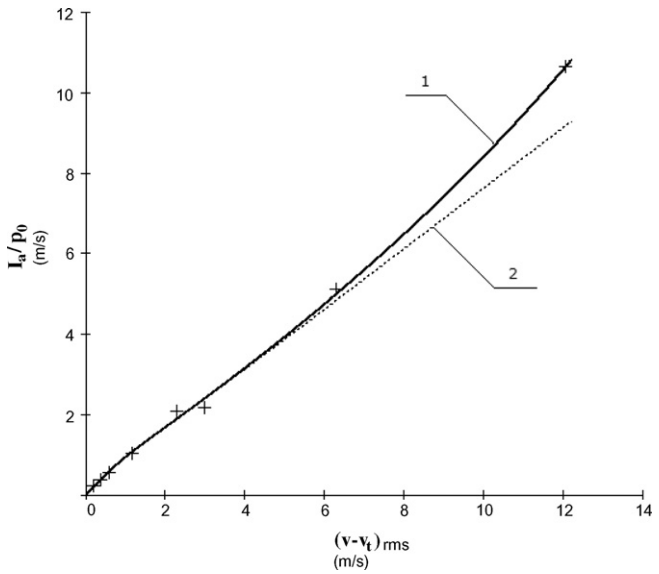

Fig. 5. Intensity of acoustic energy absorbed in water at cavitation is shown as a function of the excessive oscillatory velocity of an acoustic radiator. Line 1 is plotted from Eq. (14); line 2 is plotted from Eq. (11).

Since, as the stated theory assumes, at supercavitation the spherical shock-wave is not formed in the gas inside the bubbles, at oscillatory velocities $(v - v_t)_{rms} > 3$ m/s the characteristic changes of the secondary effects of cavitation, which are used in the sonochemical technology, must be observed.

An experimental verification of this effect was conducted by observing the cavitation-induced ultrasonic dispersion of solid particles. During the experimental setup, it was assumed that the transition to the supercavitation regime should in some way be reflected in the manner in which the dispersion occurs. The experimental study was conducted during the ultrasonic dispersion of graphite particles with the initial size 200–250 μm in settled tap water under normal conditions. To avoid any possible influence of the reactor geometry on the results of the measurements, the acoustic calorimeter described above was used as an apparatus for dispersing. For the analysis of the relative transparency of the obtained dispersions, the degree of the light absorption (at the wavelength of 420 nm) in them was measured using a photo-colorimeter. From the measurement results presented in Fig. 6 in relative units, it can be seen that the obtained curve reaches a maximum and then discontinues at $2.5 \text{ m/s} < (v - v_t)_{rms} < 3$ m/s. A subsequent smooth rise of this curve in the supercavitation region is also observed, which is most likely associated with the intense acoustic streaming, rather than with the effect of cavitation itself.

In the literature, it is indicated that the chemical action of acoustic cavitation, which is determined, for instance, from the rate of the free iodine release from the aqueous solution of potassium iodide, first increases to a certain limit with the increasing cavitation intensity and then abruptly decreases. See, for example, review [28]. In the work [25] it is experimentally shown that a rise in the rate of the release of the free iodine continues up to very high intensities of cavitation. The process rate dependence on the intensity of cavitation simply has a deep discontinuity at the transition to the supercavitation regime, which is analogous to that observed in Fig. 6. With a further increase in the radiator oscillatory velocity, the rise in the rate of the free iodine release continues.

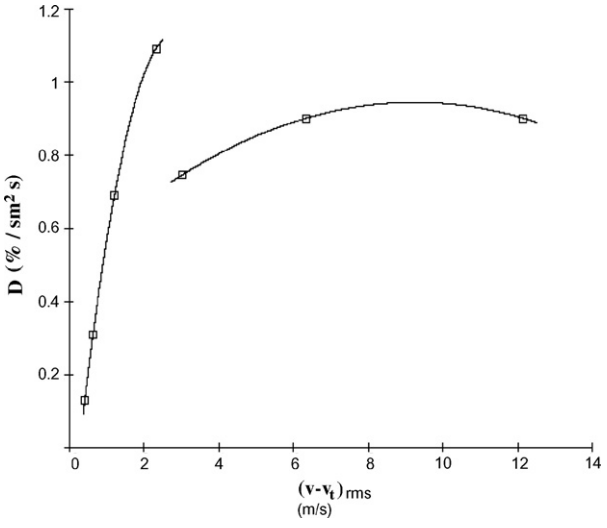

Fig. 6. Dispersing effect of acoustic cavitation (dispersion of graphite powder in water) determined by the degree of the 420 nm wavelength light absorption is illustrated as a function of the excessive oscillatory velocity of an acoustic radiator.

It appears that it is in the acoustic supercavitation region where the achievement of the highest possible temperatures during the compression of the rarefied gas inside the bubble oscillating as a Rayleigh cavity can be expected. Pressure at the bubble wall at the moment of focusing theoretically approaches infinitely high values because the gas compression is exerted by the moving dense bubble wall acting as a spherical plunger, rather than by a spherical acoustic wave [17]. In the same region, the highest intensities of the cavitation-induced sonochemical processes occurring at high temperatures may be observed. At the same time, processes connected with erosion, dispersion of solids and the like can be inhibited in the supercavitation region.

7. Conclusions

The proposed shock-wave model of acoustic cavitation reflects real events occurring in water at cavitation since calculations based on the equations that follow from the model are in good agreement with the results of the experiments. The presented experimental data extend to the region of super-high oscillatory velocities of an acoustic radiator and agree well with the theoretical model. The model makes it possible to obtain the resulting equation for the calculations of the energy absorbed by liquids during cavitation without having to consider in detail all the complex processes of the absorption of the acoustic energy, which are connected with the nonlinear oscillations of the gas bubbles during their collapse.

Within the framework of this model, the existence of a transition from the subsonic regime of acoustic cavitation to the supersonic regime is predicted. The possibility of a change in the character of the oscillations of a cavitation bubble at high values of v is theoretically shown. The conducted experimental studies confirm such a possibility.

Simple algebraic expressions that follow from the proposed model can be used in practical engineering calculations for designing powerful ultrasonic waveguide systems for sonochemical reactors following, for example, the methodology described in the work [25].

References

[1] T.G. Leighton, Ultrason. Sonochem. 2 (1995) 123.
[2] H.G. Flynn, in: W.P. Mason (Ed.), Physical Acoustics, Methods and Devices, Part B, vol. 1, Acad. Press, 1964.
[3] M.S. Plesset, A. Prosperitty, Ann. Rev. Fluid Mech. 9 (1977) 145.
[4] W. Lauterborn, C.-D. Ohl, Ultrason. Sonochem. 4 (1997) 65.
[5] J.-L. Laborde, A. Hita, J.-P. Caltagirone, A. Gerard, Ultrasonics 38 (2000) 297.

[6] G. Servant, J.L. Laborde, A. Hita, J.P. Caltagirine, A. Gerard, Ultrason. Sonochem. 8 (2001) 163.
[7] G. Servant, J.-L. Laborde, A. Hita, J.-P. Caltagirone, A. Gerard, Ultrason. Sonochem. 10 (2003) 347.
[8] W. Lauterborn, T. Kurz, R. Geisler, D. Schanz, O. Lindau, Ultrason. Sonochem. 14 (2007) 484.
[9] R. Mettin, Ph. Koch, W. Lauterborn, D. Krefting, Modeling acoustic cavitation with bubble redistribution. In: Sixth International Symposium on Cavitation CAV2006, Wageningen, The Netherlands, September 2006.
[10] J. Klima, A. Frias-Ferrer, J. Gonzalez-Garsia, J. Ludvik, V. Saez, J. Iniesta, Ultrason. Sonochem. 14 (2007) 19.
[11] R. Mettin, S. Luther, C.-D. Ohl, W. Lauterborn, Ultrason. Sonochem. 6 (1999) 25.
[12] S. Luther, R. Mettin, P. Koch, W. Lauterborn, Ultrason. Sonochem. 8 (2001) 159.
[13] J. Appel, P. Koch, R. Mettin, D. Krefting, W. Lauterborn, Ultrason. Sonochem. 11 (2004) 39.
[14] A. Moussatov, C. Granger, B. Dubus, Ultrason. Sonochem. 10 (2003) 191.
[15] A. Moussatov, R. Mettin, C. Granger, T. Tervo, B. Dubus, W. Lauterborn, WCU 2003, Paris, September 7–10, 2003.
[16] P. Diodati, G. Giannini, Ultrason. Sonochem. 8 (2001) 49.
[17] Ya. B. Zel'dovich, Yu. P. Raizer, Physics of Shock Waves and High-Temperature Hydrodynamic Phenomena, Acad. Press, New York, 1966.
[18] L. Van Vijngaarden, Annual Review of Fluid Mechanics, vol. 4, Annual Review Inc., Palo Alto, 1972, p. 369.
[19] R.A. Thuraisingham, Ultrasonics 36 (1998) 767.
[20] L.D. Rosenberg (Ed.), High-Intensity Ultrasonic Fields, Plenum Press, New York, 1971.
[21] K. Fukushima, J. Saneyoshi, Y. Kikuchi, in: Y. Kikuchi (Ed.), Ultrasonic Transducers, Corona Publ. Co., Tokyo, 1969.
[22] M.G. Salvadory, R. Skalak, P. Weidlinger, New York Acad. Sci., Div. Eng. 2 (21) (1959) 427.
[23] W. Herrmann, J. Appl. Phys. 40 (1969) 2490.
[24] A.D. Resnyansky, N.K. Bourne, J. Appl. Phys. 95 (2004) 1760.
[25] S.L. Peshkovsky, A.S. Peshkovsky, Ultrason. Sonochem. 14 (2007) 314.
[26] N.B. Brandt, A.D. Yakovlev, S.L. Peshkovsky, Russ. Tech. Phys. Lett. 1 (10) (1975) 460.
[27] R.T. Knapp, J.W. Daily, F.G. Hammitt, Cavitation, New York, 1970.
[28] T.J. Mason, Ultrason. Sonochem. 7 (2000) 145.